Journal of Radiation Research and Applied Sciences 18 (2025) 101533

Contents lists available at ScienceDirect

Journal of Radiation Research and Applied Sciences

journal homepage: www.journals.elsevier.com/journal-of-radiation-research-and-applied-sciences

In Vivo biodistribution analysis of [^{68}Ga]Ga-NOTA-pamidronic acid and [^{68}Ga]Ga-DOTA-pamidronic Acid: Insights into bone-targeting radiopharmaceuticals

Hishar Hassan [a,*], Nur Faqihah Omar Samri [b,1], Wan Hamirul Bahrin Wan Kamal [c,1], Muhamad Faiz Othman [b,**]

[a] Centre for Diagnostic Nuclear Imaging, Universiti Putra Malaysia, 43400, Serdang, Selangor, Malaysia
[b] Department of Pharmacy Practice, Faculty of Pharmacy, Universiti Teknologi MARA, 42300 Bandar Puncak Alam, Selangor, Malaysia
[c] Medical Technology Division, Malaysian Nuclear Agency (Nuclear Malaysia), 43000, Kajang, Selangor, Malaysia

ARTICLE INFO

Keywords:
[^{68}Ga]Ga-NOTA-pamidronic acid
[^{68}Ga]Ga-DOTA-pamidronic acid
Radiopharmaceuticals
Positron emission tomography (PET)
Bisphosphonate
Bone imaging

ABSTRACT

Radiolabeled bisphosphonates have shown the potential for targeted bone applications in both diagnostic imaging and therapy. In this study, we investigated the radiochemical properties and in vivo biodistribution of two novel radiopharmaceuticals; [^{68}Ga]Ga-NOTA-pamidronic acid and [^{68}Ga]Ga-DOTA-pamidronic acid, with the aim of determining their suitability for clinical applications.

Radiolabeling was achieved with a high radiochemical purity (RCP) of over 95 % for both, with [^{68}Ga]Ga-DOTA-pamidronic acid having a slightly higher RCP (99.48 %) compared to [^{68}Ga]Ga-NOTA-pamidronic acid (97.48 %). This difference emphasises the superior affinity of DOTA for binding Ga^{3+} ions, which is likely due to its structural flexibility and enhanced coordination capabilities. The biodistribution studies were performed in healthy Swiss Webster mice. Both radiopharmaceuticals showed efficient renal clearance and minimal non-specific uptake in the major organs. The kidneys and bladder showed the highest uptake, indicating renal excretion, with [^{68}Ga]Ga-DOTA-pamidronic acid showing significantly higher uptake in the bladder. However, bone uptake remained relatively low for both radiopharmaceuticals, with [^{68}Ga]Ga-NOTA-pamidronic acid showing higher uptake (1.33 %ID/g) compared to [^{68}Ga]Ga-DOTA-pamidronic acid (0.26 %ID/g). This may be attributed to rapid excretion and the possible changes in bisphosphonate binding properties due to chelation. Free ^{68}Ga showed extensive non-specific uptake, highlighting the advantages of chelated radiotracers in minimising off-target distribution.

While [^{68}Ga]Ga-NOTA-pamidronic acid and [^{68}Ga]Ga-DOTA-pamidronic acid showed promising renal clearance and minimal non-specific uptake, their bone affinity remains suboptimal. These results emphasise the need for further structural modifications to improve binding to hydroxyapatite and thus provide the basis for the development of ^{68}Ga-based radiopharmaceuticals with improved bone-targeting capabilities.

1. Introduction

Bone cancer occurs when abnormal cells multiply uncontrollably in the bone, leading to the destruction of normal bone tissue. A distinction is made between primary bone cancer, which is rare and includes sarcomas such as osteosarcoma, chondrosarcoma, Ewing's sarcoma, and chordoma, and secondary bone cancer, which is more common and arises from metastases of other primary cancers, including breast cancer (70 %), prostate cancer (85 %), lung cancer (40 %), and kidney cancer (40 %) (Coleman et al., 2020; Cosphiadi et al., 2018; Omotade et al., 2024; Oniankitan et al., 2014; Siegel et al., 2023). Secondary metastatic diseases are responsible for most cancer-related deaths and not the primary cancer itself (Sharma et al., 2021).

The diagnosis of bone cancer in nuclear medicine involves the use of radiopharmaceuticals to produce detailed images of the bone. A commonly used radiopharmaceutical is [^{18}F]NaF, a bone-seeking agent

* Corresponding author.
** Corresponding author.
E-mail addresses: muhdhishar@upm.edu.my (H. Hassan), faiz371@uitm.edu.my (M.F. Othman).
[1] Order of Co-authors.

https://doi.org/10.1016/j.jrras.2025.101533
Received 21 January 2025; Received in revised form 17 March 2025; Accepted 15 April 2025
Available online 19 April 2025

introduced by Blau et al., in 1962 and approved by the FDA in 1972 to detect osteogenic activity (Araz et al., 2015). The development of [^{18}F]NaF-PET has addressed a critical clinical challenge by enabling the identification and assessment of bone metastases (Souche et al., 2024; Wang et al., 2022).

Bisphosphonates (BPs) are pyrophosphate analogues characterised by a P-C-P core that enables strong binding to calcium in the hydroxyapatite of bone, especially in regions with high bone turnover (Mbese & Aderibigbe, 2021; Pozzi & Raje, 2011). Pamidronic acid, a nitrogen-containing bisphosphonate, has superior bone selectivity and is widely used in the imaging and treatment of bone disease (Keeling et al., 2023). Its nitrogen group makes it around 100 times more effective than previous bisphosphonates, such as etidronate and clodronate (Papapoulos, 2020).

The introduction of the ^{68}Ge/^{68}Ga generator in the early 2000s revolutionised radiopharmacy due to the beneficial properties of ^{68}Ga, including positron emission, 68-min half-life, rapid elimination and diagnostic precision (Ashhar et al., 2020; Banerjee & Pomper, 2013; Nelson et al., 2022). ^{68}Ga-labelled peptides have emerged as a new class of radiopharmaceuticals characterised by rapid target localisation and efficient blood excretion, providing an alternative to traditional ^{99m}Tc agents (Nelson et al., 2022). In contrast to covalent PET isotopes such as ^{18}F or ^{11}C, ^{68}Ga in its Ga^{3+} form requires a bifunctional chelating agent (BCA) for conjugation with target molecules. Chelators such as NOTA (1,4,7-triazacyclononane-1,4,7-triacetic acid) and DOTA (1,4,7,10-tetraazacyclododecane-1,4,7,10-tetraacetic acid) have facilitated incorporation of ^{68}Ga and enabled precise PET imaging (Shetty et al., 2010; Damerow et al., 2023; Rinne et al., 2019; Arjenaki et al., 2024).

Preliminary studies with [^{18}F]AlF-NOTA-pamidronic acid showed strong binding to hydroxyapatite and osteoblast cells in vitro (Hassan et al., 2022), supporting its potential as a radiopharmaceutical targeting bone. The aim of this study is to evaluate the in vivo biodistribution of [^{68}Ga]Ga-NOTA-pamidronic acid and [^{68}Ga]Ga-DOTA-pamidronic acid in healthy male Swiss-Webster mice to gain insight into its suitability as a diagnostic imaging agent for bone disease, as understanding its biodistribution is crucial for assessing its clinical potential.

2. Materials and methods

2.1. Materials

Pamidronic acid ($C_3H_{11}NO_7P_2$) was purchased from Santa Cruz Biotechnology (Dallas, TX, USA), while NOTA-NHS ester ($C_6H_{24}N_4O_8$) was obtained from CheMatech (Dijon, France). DOTA-NH_2 and the ^{68}Ga radionuclide were sourced from ITM ^{68}Ge/^{68}Ga generators (Munich, Germany). Other reagents included dimethylformamide (DMF), triethylamine ($C_6H_{15}N$), ammonium acetate ($NH_4CH_3CO_2$), acetic acid (CH_3COOH), formic acid (CH_2O_2), ethanol, sodium acetate ($C_2H_3NaO_2$), sodium hydroxide (NaOH), and methanol, all obtained from Sigma-Aldrich (USA) or Merck (Kenilworth, USA). Water for injection (WFI), 0.9 % sodium chloride, and isoflurane were provided by B. Braun (USA). Instant Thin Layer Chromatography-Silica Gel (ITLC-SG) plates were purchased from Agilent (Santa Clara, CA, USA), and hydrochloric acid (HCl) was used for generator elution. Instrumentation included a radioTLC imaging scanner (AR-2000, Eckert & Ziegler) and a PerkinElmer Wizard2 2470 Automatic Gamma Counter.

2.2. Methods

2.2.1. Preparation of NOTA-pamidronic acid and DOTA-pamidronic acid

Pamidronic acid was prepared by dissolving 20 mg in 2 mL of deionised water to reach a final concentration of 10 mg/mL. This prepared solution was then divided into two portions, one for the preparation of NOTA-pamidronic acid and the other for DOTA-pamidronic acid. The solution was shaken thoroughly until completely dissolved to ensure homogeneity. The pH of the solution was adjusted to 8 with 30 µL triethylamine (TEA) and monitored with pH indicator strips. Separately, 20 mg NOTA-NHS was dissolved in 1 mL dimethylformamide (DMF) and then 468.4 µL of the NOTA-NHS solution was added to the pamidronic acid solution (3:1 ratio of pamidronic acid to NOTA-NHS). For the preparation of DOTA-pamidronic acid, 20 mg DOTA-NHS was also dissolved in 1 mL DMF and approximately 540 µL of the DOTA-NHS solution was then added to the pamidronic acid solution, maintaining a similar ratio of pamidronic acid to DOTA-NHS of 3:1 as previously described. The reaction mixture was incubated 4 h at room temperature with gentle shaking in a microplate shaker and the pH was monitored hourly with pH indicator strips to ensure that it remained neutral to slightly basic.

Following the reaction, the crude NOTA-pamidronic acid and DOTA-pamidronic acid was purified to remove organic impurities. Solid phase extraction (SPE) was performed using a Sep-Pak C18 Plus Light cartridge (Waters, Milford, MA, USA), followed by filtration through a 0.22 µm nylon syringe filter (PhenexTM-NY, USA). The purified product was then validated with Liquid Chromatography Mass-Spectrometry Analysis for further use (Hassan et al., 2022).

2.2.2. Radiolabeling of [^{68}Ga]Ga-NOTA-pamidronic acid and [^{68}Ga]Ga-DOTA-pamidronic acid

The ^{68}Ga eluate was obtained from a^{68}Ge/^{68}Ga generator (ITM, Munich, Germany). Given the advanced age of the generator, the highest ^{68}Ga concentration was achieved by elution with 0.05 M HCl, discarding the first 1 mL fraction and collecting the subsequent 4 mL to minimise metallic impurities. For radiolabelling, approximately 50 µg (96.2 nmol) of NOTA-pamidronic acid in 50 µL was reacted with 1.3 ± 0.1 mCi ^{68}Ga in a total volume of 1 mL. The reaction mixture was buffered with 110 µL of 1.0 M sodium acetate (NaOAc) to achieve an optimal pH of 3.9, enabling efficient radiolabelling. The reaction was carried out at 100 °C for 15 min (Fig. 1). A similar protocol was followed for the preparation of [^{68}Ga]Ga-DOTA-pamidronic acid using 50 µg (80.5 nmol) of DOTA-pamidronic acid in 50 µL. The radiochemical purity (RCP) was determined using an instant thin layer chromatography-silica gel (iTLC-SG) plate as a stationary phase and 0.4 M acetic acid: methanol (1:1) mixture as a mobile phase and analysed using a Radio TLC-Scanner (AR-2000, Eckert & Ziegler, Berlin, Germany).

2.2.3. Biodistribution studies of [^{68}Ga]Ga-NOTA-pamidronic acid and [^{68}Ga]Ga-DOTA-pamidronic acid

Biodistribution studies were performed with 12 healthy male Swiss-Webster mice (12–16 weeks old, 35–40 g), with three animals assigned to each experimental group: free ^{68}Ga, [^{68}Ga]Ga-NOTA-pamidronic acid and [^{68}Ga]Ga-DOTA-pamidronic acid. Analyses were performed at two time points: 15 min and 30 min after injection. The mice were kept in ventilated cages under standard laboratory conditions and had ad libitum access to food and water.

For the experimental procedure, mice were anaesthetised with isoflurane and 0.4 mL (30.4 ± 22.9 µCi) [^{68}Ga]Ga-NOTA-pamidronic acid was administered intravenously via the tail vein. 30 min after injection, the mice were euthanised by exsanguination of the heart (Aguwa et al., 2020). The organs of interest, including liver, spleen, kidney, muscle, femur, lung, heart, blood, stomach and intestine, were carefully harvested, weighed and analysed for radioactivity using a PerkinElmer Wizard2 2470 automated gamma counter. Biodistribution results were expressed as percentage of injected dose per gramme of tissue (%ID/g) (Arjenaki et al., 2024; Silva et al., 2022; Hu et al., 2022). The protocol was applied in a similar way for [^{68}Ga]Ga-DOTA-pamidronic acid and free ^{68}Ga, following identical steps for injection, euthanasia, organ harvesting and radioactivity measurement. The in vivo study was performed with approval from the Committee on Animal Research and Ethics (CARE), Universiti Teknologi MARA, authorization no. UiTM CARE: 442/2024 (600-UiTMCARE(PT.1/3/1)).

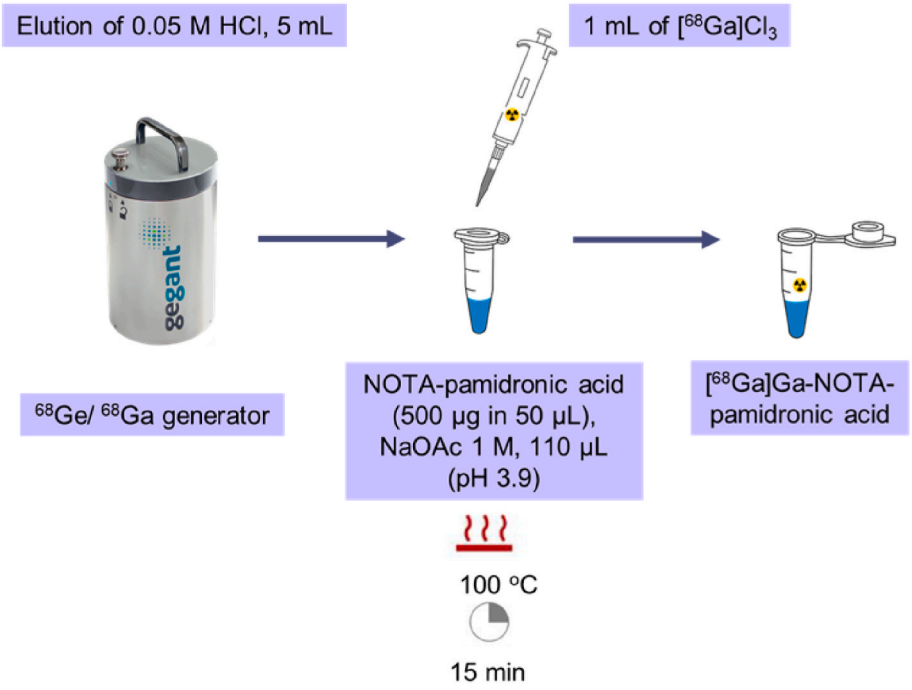

Fig. 1. Workflow illustration for radiolabeling of [^{68}Ga]Ga-NOTA-pamidronic acid.

3. Results and discussion

3.1. Radiolabeling of [^{68}Ga]Ga-NOTA-pamidronic acid and [^{68}Ga]Ga-DOTA-pamidronic acid

For the radiolabeling of [^{68}Ga]Ga-NOTA-pamidronic acid and [^{68}Ga]Ga-NOTA-pamidronic acid, the i-TLC result showed that both [^{68}Ga]Ga-NOTA-pamidronic acid and [^{68}Ga]Ga-DOTA-pamidronic acid achieved excellent radiolabeling purity (RCP), with values above the 95 % threshold required for clinical applications (Table 1). [^{68}Ga]Ga-DOTA-pamidronic acid consistently showed higher RCP values, 99.5 % ± 0.01 ($n = 3$) compared to [^{68}Ga]Ga-NOTA-pamidronic acid, (97.5 % ± 0.09 ($n = 3$), indicating a more efficient radiolabeling process. This higher RCP value ensures accurate dosing and optimal results in imaging and therapy.

The retention factors (R_f) of both compounds were similar, indicating comparable physical and chemical properties after labelling (Fig. 2). While both compounds exhibit high RCP and stability, the slightly higher RCP of [^{68}Ga]Ga-DOTA-pamidronic acid highlights its potential preference for applications demanding higher purity, such as high-resolution imaging or precise therapeutic dosing.

The observed differences in radiolabelling efficiency can be attributed to the structural properties of the chelators. DOTA is widely recognised for its superior binding affinity with ^{68}Ga. This is due to its cyclic structure with four carboxylic acid arms, which provides multiple coordination sites that enhance metal-chelator interactions and stability. The larger ring structure of DOTA offers a flexible geometry that facilitates efficient coordination with ^{68}Ga, making it the most commonly used chelator in the development of metal radiopharmaceuticals (Davey & Paterson, 2023). Its versatility, in vivo stability and the availability of bifunctional derivatives emphasise its utility (Souche et al., 2024).

Conversely, NOTA has distinct advantages, particularly in diagnostic applications (Lee et al., 2023). A study by Käkelä (2020) summarised other studies and highlighted the rapid reaction kinetics, high in vivo stability, efficient radiolabelling at room temperature and strong selectivity for ^{68}Ga offered by NOTA chelators (Käkelä, 2020). The cavity size of NOTA-based ligands is perfectly suited for trivalent gallium (Ga^{3+}). They form thermodynamically stable complexes without the distorted octahedral structure observed in DOTA-based Ga^{3+} complexes (Kubíček et al., 2010). These properties make NOTA an excellent choice for medical imaging applications where diagnostic accuracy is paramount.

Nevertheless, the physicochemical properties of [^{68}Ga]Ga-NOTA-pamidronic acid and [^{68}Ga]Ga-DOTA-pamidronic acid, such as hydrophilicity (log P values) and in vivo stability, were not investigated in this study. These properties could influence the affinity of the compounds for bone and overall pharmacokinetics. Future research should incorporate these analyses to further enlighten the effects of chelation on biodistribution and binding properties. Despite these limitations, the study provides valuable preliminary data on the in vivo biodistribution of ^{68}Ga-labelled bisphosphonates and serves as a basis for further refinement and evaluation in disease-specific models.

In summary, both [^{68}Ga]Ga-NOTA-pamidronic acid (Fig. 3) and [^{68}Ga]Ga-DOTA-pamidronic acid (Fig. 4) exhibit excellent radiolabelling efficiency and stability. The higher RCP of [^{68}Ga]Ga-DOTA-pamidronic acid may make it more suitable for applications where radiochemical purity is critical. The use of i-TLC provided valuable preliminary data on radiolabelling conditions and highlighted the complementary role of DOTA and NOTA chelators in the development of radiopharmaceuticals.

Table 1
RCP of [^{68}Ga]Ga-NOTA-pamidronic acid and [^{68}Ga]Ga-DOTA-pamidronic acid.

Radiopharmaceutical	%RCP ($n = 3$)	Retention factor (R_f) ($n = 3$)
[^{68}Ga]Ga-NOTA-pamidronic acid	97.5 (±0.09)	0.949 (±0.001)
[^{68}Ga]Ga-DOTA-pamidronic acid	99.5 (±0.01)	0.951 (±0.003)

3.2. Biodistribution studies of [^{68}Ga]Ga-NOTA-pamidronic acid and [^{68}Ga]Ga-DOTA-pamidronic acid

The biodistribution study investigated the tissue distribution of [^{68}Ga]Ga-NOTA-pamidronic acid, [^{68}Ga]Ga-DOTA-pamidronic acid and free ^{68}Ga in healthy male Swiss-Webster mice (n=3 per group). The percentage of injected dose per gram of tissue (%ID/g) was determined

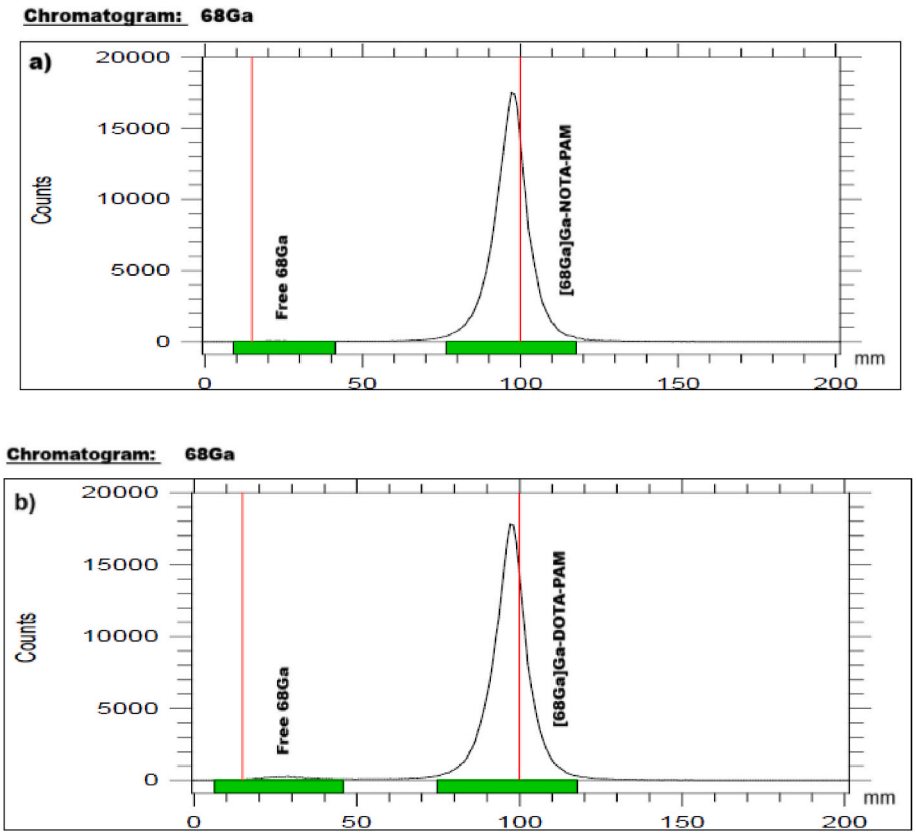

Fig. 2. RCP analysis for (**a**) [^{68}Ga]Ga-NOTA-pamidronic acid, and (**b**) [^{68}Ga]Ga-DOTA-pamidronic acid using iTLC-SG plate and 0.4 M acetic acid: methanol (1:1) as the mobile phase.

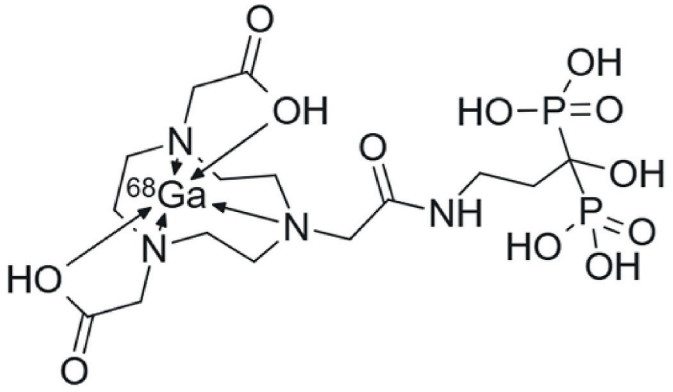

Fig. 3. The structure of radiolabeled [^{68}Ga]Ga-NOTA-pamidronic acid.

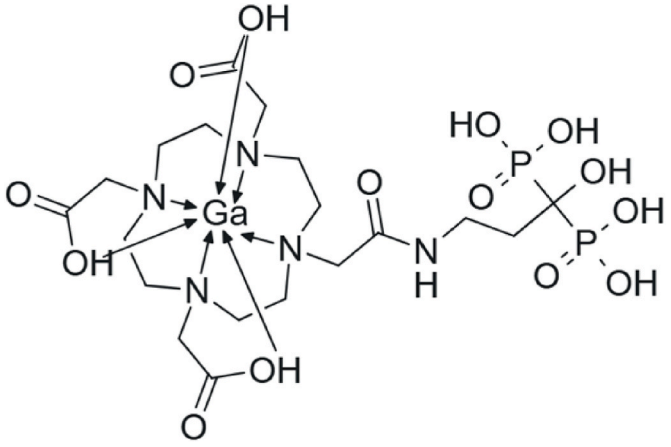

Fig. 4. The structure of radiolabeled [^{68}Ga]Ga-DOTA-pamidronic acid.

30 min after injection to determine pharmacokinetic profiles and organ-specific uptake. The results, presented in Table 2, provide a comparative analysis of the radiotracers and highlight the differences in uptake and clearance patterns between organs. This comparison provides insight into the potential suitability of the radiotracers for bone-targeting applications.

Free ^{68}Ga showed significantly higher uptake in most organs, including the liver (5.32 ± 1.04 %ID/g), spleen (6.35 ± 1.66 %ID/g), kidneys (10.21 ± 0.68 %ID/g), lungs (14.31 ± 4.11 %ID/g), heart (10.37 ± 2.53 %ID/g) and blood (33.71 ± 3.15 %ID/g) (Table 2). This non-specific biodistribution indicates that free ^{68}Ga remained largely unbound, resulting in extensive retention in highly perfused tissue and low clearance. The increased activity in the blood also suggests that a significant proportion of free ^{68}Ga circulates unbound and is only taken up to a limited extent by certain organs.

In contrast, both [^{68}Ga]Ga-NOTA-pamidronic acid and [^{68}Ga]Ga-DOTA-pamidronic acid showed significantly lower uptake in most tissues, highlighting the efficacy of chelation in reducing non-specific binding and improving clearance (Fig. 5). The highest uptake of [^{68}Ga]Ga-NOTA-pamidronic acid was observed in the kidneys (2.63 ± 0.70 %ID/g), followed by the bone (1.33 ± 0.16 %ID/g), indicating a predominant renal excretion while maintaining some affinity for hydroxyapatite in bone. A similar pattern was observed for [^{68}Ga]Ga-DOTA-pamidronic acid, with the highest uptake in the kidneys (3.60 ± 1.11 %ID/g), although uptake in bone remained low (0.26 ± 0.08 %ID/g). These results suggest that both tracers undergo rapid renal clearance, with [^{68}Ga]Ga-NOTA-pamidronic acid exhibiting slightly higher bone retention compared to its DOTA-conjugated counterpart.

Table 2
The %ID/g of related organs for [^{68}Ga]Ga-NOTA-pamidronic acid, [^{68}Ga]Ga-DOTA-pamidronic acid and free ^{68}Ga 30 min p.i

Organs	[^{68}Ga]Ga-NOTA-pamidronic acid	Free ^{68}Ga	[^{68}Ga]Ga-DOTA-pamidronic acid
Liver	0.48 ± 0.17	5.32 ± 1.04	0.36 ± 0.14
Spleen	0.14 ± 0.08	6.35 ± 1.66	0.26 ± 0.20
Kidneys	2.63 ± 0.70	10.21 ± 0.68	3.60 ± 1.11
Muscle	0.13 ± 0.02	2.79 ± 0.86	0.27 ± 0.17
Bone	1.33 ± 0.16	5.18 ± 1.93	0.26 ± 0.08
Lungs	0.32 ± 0.06	14.31 ± 4.11	0.58 ± 0.43
Heart	0.11 ± 0.01	10.37 ± 2.53	0.28 ± 0.29
Blood	0.27 ± 0.07	33.71 ± 3.15	0.68 ± 0.26
Stomach	0.09 ± 0.02	5.39 ± 1.31	0.21 ± 0.17
Gut	0.14 ± 0.02	6.40 ± 2.80	0.38 ± 0.33

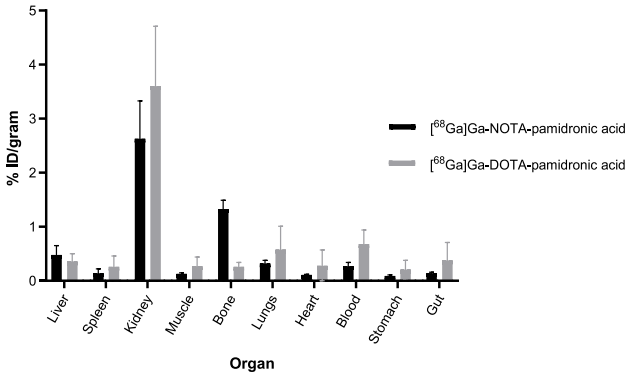

Fig. 5. The in vivo biodistribution study between [^{68}Ga]Ga-NOTA-pamidronic acid and [^{68}Ga]Ga-DOTA-pamidronic acid 30 min p.i.

Both [^{68}Ga]Ga-NOTA-pamidronic acid and [^{68}Ga]Ga-DOTA-pamidronic acid showed relatively low bone uptake, with [^{68}Ga]Ga-NOTA-pamidronic acid showing slightly higher uptake (1.33 ± 0.16 %ID/g) compared to [^{68}Ga]Ga-DOTA-pamidronic acid (0.26 ± 0.08 %ID/g). This was unexpected given the well-documented high bone affinity of bisphosphonates in a previous study (Meckel et al., 2017). Several factors may explain this discrepancy. Firstly, the rapid renal clearance of both substances may limit the time available for binding to bone tissue. This could be due to the ionic structure of [^{68}Ga]Ga-NOTA-pamidronic acid and [^{68}Ga]Ga-DOTA-pamidronic acid, which may favour excretion over a longer retention time in bone, which has been observed particularly for [^{68}Ga]Ga-DOTA-pamidronic acid (Ashhar et al., 2020). Secondly, chelation of pamidronic acid by NOTA or DOTA may alter its binding properties and reduce its affinity for hydroxyapatite in bone compared to the non-chelated form. The observed difference in uptake between the two tracers suggests that the choice of chelating agent may influence targeting accuracy in bone, possibly due to variations in charge distribution and steric effects.

To further investigate the time-dependent distribution of [^{68}Ga]Ga-NOTA-pamidronic acid, biodistribution was analysed at 15 and 30 min after injection (Table 3). Due to experimental limitations, a similar time course analysis was not possible for [^{68}Ga]Ga-DOTA-pamidronic acid; however, the data provide insight into the early pharmacokinetics of [^{68}Ga]Ga-NOTA-pamidronic acid. The temporal biodistribution data of [^{68}Ga]Ga-NOTA-pamidronic acid showed progressive accumulation in most organs between 15 and 30 min after injection, with marked uptake in the kidneys (9.27 ± 2.57 %ID/g), confirming efficient renal clearance (Table 3). A slight increase in uptake over time was also observed in liver, lung, blood, stomach and intestine, suggesting continued systemic distribution and slower clearance from these tissues. Uptake into bone showed a modest increase from 0.29 ± 0.15 %ID/g at 15 min to 1.33 ± 0.16 %ID/g at 30 min, indicating a limited but delayed affinity for bone tissue (Fig. 6).

Table 3
The in vivo biodistribution of [^{68}Ga]Ga-NOTA-pamidronic acid in healthy male Swiss-Webster mice, %ID/gram for organ of interest, 15- and 30-min p.i

Organs	15 min	30 min
Liver	1.14 ± 0.16	0.48 ± 0.17
Spleen	0.09 ± 0.09	0.14 ± 0.08
Kidney	9.27 ± 2.57	2.63 ± 0.70
Muscle	0.81 ± 0.11	0.13 ± 0.02
Bone	0.29 ± 0.15	1.33 ± 0.16
Lungs	1.98 ± 0.59	0.32 ± 0.06
Heart	0.94 ± 0.37	0.11 ± 0.01
Blood	2.63 ± 0.96	0.27 ± 0.07
Stomach	1.28 ± 0.66	0.09 ± 0.02
Gut	0.83 ± 0.26	0.14 ± 0.02

This study demonstrated the successful radiolabeling of NOTA- and DOTA-conjugated pamidronic acid with ^{68}Ga, providing important insights into their in vivo biodistribution. Both radiotracers exhibited high radiochemical purity (RCP) and efficient renal clearance, confirming their suitability for further evaluation as radiopharmaceuticals for bone. However, the expected high bone uptake characteristic of bisphosphonates was not observed. This unexpected finding indicates possible limitations in the binding affinity of these radiotracers and suggests that chelation with NOTA and DOTA may affect the interaction between pamidronic acid and hydroxyapatite in bone tissue. A similar effect was observed in Pfannkuchen et al., who reported significant improvements in the blood-bone ratio when they added various chelating agents to zoledronic acid (Pfannkuchen et al., 2017).

Several ^{68}Ga-labelled bisphosphonates have been investigated for bone imaging, including [^{68}Ga]Ga-DOTA-bisphosphonate ligand BPAPD ([^{68}Ga]Ga-BPAPD), [^{68}Ga]Ga-NODAGA-pamidronic acid and [^{68}Ga]Ga-DOTA-zoledronic acid ([^{68}Ga]Ga-DOTA-ZOL), which have shown high accumulation in the bone and rapid excretion in the blood (Ashhar et al., 2020; Meckel et al., 2016). Compared to these tracers, [^{68}Ga]Ga-NOTA-pamidronic acid and [^{68}Ga]Ga-DOTA-pamidronic showed relatively lower bone uptake despite their structural similarity to other bisphosphonate-based agents. For example, [^{68}Ga]Ga-BPAPD was reported to have a bone uptake of 3.21 ± 0.62 %ID/g, 60 min after injection, while [^{68}Ga]Ga-DOTA-ZOL showed better hydroxyapatite binding due to its higher charge density and rigid chelate structure (5.40 ± 0.62 %ID/g). In contrast, in this study, [^{68}Ga]Ga-NOTA-pamidronic acid and [^{68}Ga]Ga-DOTA-pamidronic acid showed relatively low bone uptake (1.33 ± 0.16 %ID/g and 0.26 ± 0.08 %ID/g, respectively, 30

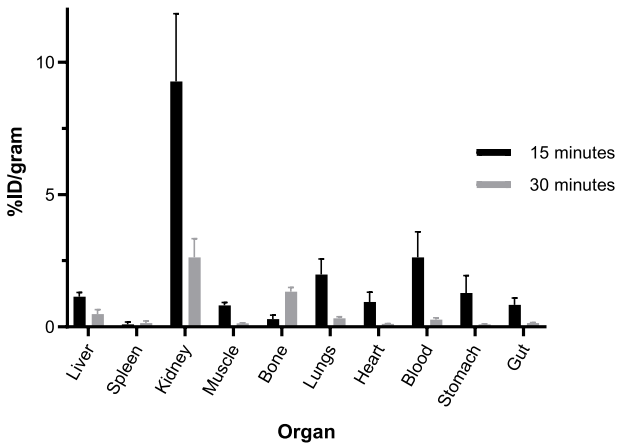

Fig. 6. In vivo biodistribution of [^{68}Ga]Ga-NOTA-pamidronic acid at 15- and 30- minutes p.i.

min after injection).

One possible explanation for this difference is that the chemistry of the chelates significantly influences bone affinity (Ashhar et al., 2020). DOTA and NOTA chelators lead to different charge distributions, which may alter the overall hydrophilicity of the radiotracer and affect its binding to hydroxyapatite. While previous studies suggest that NODAGA-based bisphosphonates ([^{68}Ga]Ga-NODAGA-pamidronic acid) have better bone uptake due to a more favourable charge to lipophilicity ratio, Ashhar et al., found no improvement in bone affinity with [^{68}Ga]Ga-NODAGA-pamidronic acid compared to [68Ga]Ga-DOTA-pamidronic acid (Ashhar et al., 2020; Meckel et al., 2016).

In contrast, our study showed that [^{68}Ga]Ga-NOTA-PAM had a significantly higher %ID/g in bone compared to [^{68}Ga]Ga-DOTA-PAM 30 min after injection ($p < 0.05$). This suggests that the NOTA chelator may have better bone retention properties than DOTA in conjunction with pamidronic acid. The observed difference emphasises the potential influence of chelator selection on bone targeting efficiency and warrants further investigation of the underlying mechanisms.

Another factor contributing to the lower bone uptake observed in this study could be the differences in molar activity and precursor concentration. In previous studies with [^{68}Ga]Ga-DOTA-ZOL and [^{68}Ga]Ga-BPAPD, lower precursor amounts (25 nmol) were used, which increased molar activity and possibly allowed for greater binding affinity to hydroxyapatite (Meckel et al., 2016). In contrast, 80–100 nmol of precursors (NOTA-pamidronic acid and DOTA-pamidronic acid) was used in this study, which may have resulted in lower molar activity, possibly leading to receptor saturation effect and reducing the fraction of radiotracer available for bone binding. Higher precursor concentration may also increase non-specific binding and faster renal clearance, further limiting accumulation in the skeleton (Lever et al., 2017). This may explain the lower %ID/g in bone observed in our study, highlighting the need for further optimisation of precursor concentration to improve targeting accuracy in bone.

The results show important differences in the pharmacokinetics of free ^{68}Ga, [^{68}Ga]Ga-NOTA-pamidronic acid and [^{68}Ga]Ga-DOTA-pamidronic acid. While free ^{68}Ga exhibited widespread non-specific distribution and prolonged retention, both chelated compounds showed improved clearance profiles with minimal non-specific uptake. However, the relatively low bone uptake for both [^{68}Ga]Ga-NOTA-pamidronic acid and [^{68}Ga]Ga-DOTA-pamidronic acid highlights the need for further optimisation to improve the properties of the bone target. Despite these limitations, the efficient renal clearance and in vivo stability of [^{68}Ga]Ga-NOTA-pamidronic acid suggest its potential as a theranostic agent, provided that further modifications improve its bone specificity.

3.3. Limitation of the study

This study has some limitations that should be considered when interpreting the results. Firstly, the use of healthy mice instead of a bone cancer model may have influenced the observed biodistribution patterns. Due to budgetary constraints, this preliminary investigation focused on evaluating the basic pharmacokinetics of [^{68}Ga]Ga-NOTA-pamidronic acid and [^{68}Ga]Ga-DOTA-pamidronic acid rather than disease-specific targeting. Future studies should use bone tumour models to better assess the specificity and clinical relevance of these radiotracers.

Secondly, biodistribution analysis was only performed at two early time points (15 and 30 min after-injection), which limits the understanding of long-term retention and clearance of the tracer. A more comprehensive time course study with extended time points would allow a better understanding of the stability and accumulation of the radiotracer in the bone tissue.

Thirdly, important physicochemical properties such as hydrophilicity (log P values) and in vivo stability were not assessed. These factors play a crucial role in the affinity of bisphosphonate-based radiotracers for bone and their overall biodistribution. Future studies should incorporate these analyses to determine the effects of chelation on bone efficacy. Despite these limitations, this study provides valuable preliminary data on the in vivo biodistribution of ^{68}Ga-labelled pamidronate derivatives and establishes a basis for further optimisation.

4. Conclusion

This study investigated the radiolabelling efficiency and biodistribution of [^{68}Ga]Ga-NOTA-pamidronic acid and [^{68}Ga]Ga-DOTA-pamidronic acid and demonstrated their high RCP and efficient renal clearance. However, the expected high bone uptake was not observed, suggesting that chelation of pamidronic acid with NOTA and DOTA may alter the binding affinity to hydroxyapatite. This unexpected result underlines the need for further structural modifications to improve bone specificity while maintaining favourable pharmacokinetics.

Despite the limitations of the study, which include the use of healthy mice and a short biodistribution window, the results provide important insights into the pharmacokinetics and excretion profiles of these radiotracers. Future research should focus on evaluating these compounds in bone cancer models, extending the biodistribution time points and evaluating the physicochemical properties to optimise their diagnostic and therapeutic potential. These improvements will be essential for the conversion of ^{68}Ga-labelled bisphosphonates into clinically useful radiopharmaceuticals targeting bone.

CRediT authorship contribution statement

Hishar Hassan: Writing – review & editing, Supervision, Resources, Conceptualization. **Nur Faqihah Omar Samri:** Writing – original draft, Formal analysis. **Wan Hamirul Bahrin Wan Kamal:** Writing – review & editing, Supervision, Resources. **Muhamad Faiz Othman:** Writing – review & editing, Supervision, Conceptualization.

Institutional review board statement

The in vivo study was performed with approval from the Committee on Animal Research and Ethics (CARE), Universiti Teknologi MARA, authorization no. UiTM CARE: 442/2024 (600-UiTMCARE(PT.1/3/1)).

Conflict of interest

The authors declare no conflicts of interest regarding this article.

Acknowledgement

The authors extend their appreciation to Laboratory Animal Facility and Management (LAFAM) of Universiti Teknologi MARA (UiTM), Universiti Putra Malaysia (UPM) and Malaysian Nuclear Agency for supporting this work. This work was supported by Universiti Putra Malaysia(UPM) through Putra Grant (9775200).

References

Aguwa, U. S., Eze, C. E., Obinwa, B. N., Okeke, S. N., Onwuelingo, S. F., Okonkwo, D. I., Ogbuokiri, D. K., Agulanna, A. E., Obiesie, I. J., & Umezulike, A. J. (2020). Comparing the effect of methods of rat euthanasia on the brain of wistar rats: Cervical dislocation, chloroform inhalation, diethyl ether inhalation and formalin inhalation. *Journal of Advances in Medicine and Medical Research, 32*(17), 8–16. https://doi.org/10.9734/jammr/2020/v32i1730636

Araz, M., Aras, G., & Küçük, Ö. N. (2015). The role of 18F-NaF PET/CT in metastatic bone disease. *Journal of Bone Oncology, 4*(3), 92–97. https://doi.org/10.1016/j.jbo.2015.08.002

Arjenaki, G., Raziyeh, Samieepour, G., Ebrahimi, S. E. S., Hamedani, M. P., Saffari, M., Seyedhamzeh, M., Kamali, A. N., Najdian, A., & Ardestani, M. S. (2024). Development of novel radiolabeled antibody-conjugated graphene quantum dots for targeted in vivo breast cancer imaging and biodistribution studies. *Arabian Journal of Chemistry, 17*(2), Article 105518. https://doi.org/10.1016/j.arabjc.2023.105518

Ashhar, Z., Yusof, N. A., Saad, F. F. A., Nor, S. M. M., Mohammad, F., Kamal, W. H. B. W., Hassan, M. H., Hazlina, A. H., & Al-Lohedan, H. A. (2020). Preparation, characterization, and radiolabeling of [(68)Ga]Ga-NODAGA-Pamidronic acid: A potential PET bone imaging agent. *Molecules, 25*(11), 2668. https://doi.org/10.3390/molecules25112668

Banerjee, S. R., & Pomper, M. G. (2013). Clinical applications of gallium-68. *Applied Radiation and Isotopes: Including Data, Instrumentation and Methods for Use in Agriculture, Industry and Medicine, 76*(June), 2–13. https://doi.org/10.1016/j.apradiso.2013.01.039

Coleman, R., Hadji, P., Body, J.-J., Santini, D., Chow, E., Terpos, E., Oudard, S., Bruland, Ø., Flamen, P., Kurth, A., Van Poznak, C., Aapro, M., & Jordan, K. (2020). Bone health in cancer: ESMO clinical Practice guidelines. *Annals of Oncology: Official Journal of the European Society for Medical Oncology, 31*(12), 1650–1663. https://doi.org/10.1016/j.annonc.2020.07.019

Cosphiadi, I., Atmakusumah, T. D., Siregar, N. C., Muthalib, A., Harahap, A., & Mansyur, M. (2018). Bone metastasis in advanced breast cancer: Analysis of gene expression microarray. *Clinical Breast Cancer, 18*(5), e1117–e1122. https://doi.org/10.1016/j.clbc.2018.03.001

Damerow, H., Wängler, B., Schirrmacher, R., Fricker, G., & Wängler, C. (2023). Synthesis of a bifunctional cross-bridged chelating agent, peptide conjugation, and comparison of 68Ga labeling and complex stability characteristics with established chelators. *ChemMedChem, 18*(1), Article e202200495. https://doi.org/10.1002/cmdc.202200495

Davey, P. R. W. J., & Paterson, B. M. (2023). Modern developments in bifunctional chelator design for gallium radiopharmaceuticals. *Molecules*. https://doi.org/10.3390/molecules28010203

Hassan, H., Othman, M. F., Abdul Razak, H. R., Zakaria, Z. A., Saad, F. F. A., Osman, M. A., Yi, L. H., Ashhar, Z., Idris, J., Abdul Hamid, M. H. N., & Safee, Z. M. (2022). Preparation, optimisation, and in vitro evaluation of [18F]AlF-NOTA-Pamidronic acid for bone imaging PET. *Molecules*. https://doi.org/10.3390/molecules27227969

Hu, K., Li, J., Wang, L., Huang, Y., Li, L., Ye, S., Han, Y., Huang, S., Wu, H., Su, J., & Tang, G. (2022). Preclinical evaluation and pilot clinical study of [18F]AlF-labeled FAPI-tracer for PET imaging of cancer associated fibroblasts. *Acta Pharmaceutica Sinica B, 12*(2), 867–875. https://doi.org/10.1016/j.apsb.2021.09.032

Käkelä, M. (2020). Gallium-68 radiolabeling of biomolecules for positron emission tomography with special reference to imaging of inflammation and bone. https://api.semanticscholar.org/CorpusID:213433498.

Keeling, G. P., Friedrich, B., Katsamenis, O. L., Xue, J., Blower, P. J., Bertazzo, S., & Rosales, R. T M de (2023). (68)Ga-Bisphosphonates for the imaging of extraosseous calcification by positron emission tomography. *Scientific Reports, 13*(1), Article 14611. https://doi.org/10.1038/s41598-023-41149-7

Kubíček, V., Havlíčková, J., Kotek, J., Tircsó, G., Hermann, P., Tóth, É., & Lukeš, I. (2010). Gallium(III) complexes of DOTA and DOTA−Monoamide: Kinetic and thermodynamic studies. *Inorganic Chemistry, 49*(23), 10960–10969. https://doi.org/10.1021/ic101378s

Lee, I., Kim, M. H., Lee, K., Oh, K., Lim, H., Ahn, J. H., Lee, Y. J., Jeong Cheon, G., Yoon Chi, D., & Lim, S. M. (2023). Comparison of the effects of DOTA and NOTA chelators on 64Cu-cudotadipep and 64Cu-cunotadipep for prostate cancer. *Diagnostics, 13*(16). https://doi.org/10.3390/diagnostics13162649

Lever, S. Z., Fan, K.-H., & Lever, J. R. (2017). Tactics for preclinical validation of receptor-binding radiotracers. *Nuclear Medicine and Biology, 44*(January), 4–30. https://doi.org/10.1016/j.nucmedbio.2016.08.015

Mbese, Z., & Aderibigbe, B. A. (2021). Bisphosphonate-based conjugates and derivatives as potential therapeutic agents in osteoporosis, bone cancer and metastatic bone cancer. *International Journal of Molecular Sciences, 22*(13). https://doi.org/10.3390/ijms22136869

Meckel, M., Bergmann, R., Miederer, M., & Roesch, F. (2016). Bone targeting compounds for radiotherapy and imaging: *Me(III)-DOTA conjugates of bisphosphonic acid, pamidronic acid and zoledronic acid. *EJNMMI Radiopharmacy and Chemistry, 1*(1), 14. https://doi.org/10.1186/s41181-016-0017-1

Meckel, M., Bergmann, R., Miederer, M., & Roesch, F. (2017). Bone targeting compounds for radiotherapy and imaging: *Me(III)-DOTA conjugates of bisphosphonic acid, pamidronic acid and zoledronic acid. *EJNMMI Radiopharmacy and Chemistry, 1*(1), 14. https://doi.org/10.1186/s41181-016-0017-1

Nelson, B. J. B., Andersson, J. D., Wuest, F., & Spreckelmeyer, S. (2022). Good practices for 68Ga radiopharmaceutical production. *EJNMMI Radiopharmacy and Chemistry, 7*(1), 27. https://doi.org/10.1186/s41181-022-00180-1

Omotade, A., Malhotra, A., & Holloway, B. (2024). Complete fatty replacement of lytic bone metastases following treatment. A case report, assessing response to treatment of bone metastases on CT imaging. *Radiology Case Reports, 19*(1), 455–458. https://doi.org/10.1016/j.radcr.2023.09.044

Oniankitan, O., Kakpovi, K., Kpoti, M., Houzou, P., Fianyo, E., Koffi-Tessio, V. E. S., Tagbor, K. C., & Mijiyawa, M. (2014). Profile of secondary bone cancer in Lomé (Togo). *Open Journal of Rheumatology and Autoimmune Diseases, 4*, 192–197. https://api.semanticscholar.org/CorpusID:37922768.

Papapoulos, S. E. (2020). Pamidronate: A model compound of the pharmacology of nitrogen-containing bisphosphonates; A leiden historical perspective. *Bone, 134*(May), Article 115244. https://doi.org/10.1016/j.bone.2020.115244

Pfannkuchen, N., Bergmann, R., Pietzsch, J., Bachmann, M., & Roesch, F. (2017). DOTA^{ZOL}and NODAGA^{ZOL} for theranostics of bone metastases. *Journal of Nuclear Medicine, 58*(supplement 1), 324 LP– 324 http://jnm.snmjournals.org/content/58/supplement_1/324.abstract.

Pozzi, S., & Raje, N. (2011). The role of bisphosphonates in multiple myeloma: Mechanisms, side effects, and the future. *The Oncologist, 16*(5), 651–662. https://doi.org/10.1634/theoncologist.2010-0225

Rinne, S. S., Leitao, C. D., Gentry, J., Mitran, B., Abouzayed, A., Tolmachev, V., Ståhl, S., Löfblom, J., & Orlova, A. (2019). Increase in negative charge of 68Ga/chelator complex reduces unspecific hepatic uptake but does not improve imaging properties of HER3-targeting affibody molecules. *Scientific Reports, 9*(1), Article 17710. https://doi.org/10.1038/s41598-019-54149-3

Sharma, A., Prasad Yadav, D., Garg, H., Kumar, M., Sharma, B., & Koundal, D. (2021). Bone cancer detection using feature extraction based machine learning model. *Computational and Mathematical Methods in Medicine, 2021*, Article 7433186, 13 pages, 2021 https://api.semanticscholar.org/CorpusID:245368875.

Shetty, D., Lee, Y.-S., & Jeong, J. M. (2010). (68)Ga-Labeled radiopharmaceuticals for positron emission tomography. *Nuclear Medicine and Molecular Imaging, 44*(4), 233–240. https://doi.org/10.1007/s13139-010-0056-6

Siegel, R. L., Kimberly, D. M., Wagle, N. S., & Jemal, A. (2023). Cancer statistics, 2023. *CA: A Cancer Journal for Clinicians, 73*(1), 17–48. https://doi.org/10.3322/caac.21763

Silva, L. De, Fu, J.-Y., Htar, T. T., Kamal, W. H. B. W., Kasbollah, A., Muniyandy, S., & Chuah, L.-H. (2022). Biodistribution study of niosomes in tumor-implanted BALB/C mice using scintigraphic imaging. *Frontiers in Pharmacology, 12*. https://doi.org/10.3389/fphar.2021.778396

Souche, C., Fouillet, J., Rubira, L., Donzé, C., Deshayes, E., & Fersing, C. (2024). Bisphosphonates as radiopharmaceuticals: Spotlight on the development and clinical use of DOTAZOL in diagnostics and palliative radionuclide therapy. *International Journal of Molecular Sciences, 25*(1). https://doi.org/10.3390/ijms25010462

Wang, D., Li, H. W., Guo, C. M., Huang, S., Guo, X. F., & Xiao, J. X. (2022). The value of (18)F-NaF PET/CT in the diagnosis of bone metastases in patients with nasopharyngeal carcinoma using visual and quantitative analyses. *Frontiers in Bioengineering and Biotechnology, 10*, Article 949480. https://doi.org/10.3389/fbioe.2022.949480